High performance 60-GHz dielectric rod antenna with dual circular polarization

High Performance 60-GHz Dielectric Rod Antenna with Dual Circular Polarization

M.W. Rousstia and M.H.A.J. Herben
Eindhoven University of Technology, The Netherlands
E-mail: {m.w.rousstia, m.h.a.j.herben}@tue.nl

***Abstract*—In this paper, the design of a high performance dielectric rod antenna is described and validated through measurements. The manufactured 60-GHz dielectric rod antenna has the predicted gain of around 15 dBi and supports dual circular polarization. The lateral dimension of the rod antenna is very small in comparison to its counterparts. The measured port-to-port isolation larger than 20 dB is obtained for the bandwidth of 1.1 GHz. The measured axial ratio (*AR*) in the bandwidth of interest is below 0.5 dB. It will be shown that the very wideband return loss is due to the quadrature hybrid coupler.**

***Index Terms*—Dielectric rod, millimeter-wave antenna, 60 GHz, quadrature hybrid coupler, circular polarization.**

I. Introduction

IN consumer, industrial and automotive areas, the need for high data rate communication inevitably increases. The use of wireless communication has also rapidly increased, much faster than its wireline counterpart. As a result, the required bandwidth doubles every 18 months [1]. Moreover, the number of wireless devices owned per user has been ever increasing. Not only will the wireless devices connect people to people, but also people to machines and machines to machines. Nevertheless, the Industrial, Scientific, Medical (ISM) application band at 2.4 GHz has been overcrowded by numerous commercial products of end users. The availability of 7 GHz (US) and 9 GHz (Europe) around 60 GHz (ISM-band) is able to accommodate high data rate and dense local wireless communication. Furthermore, the propagation condition in the 60-GHz wireless channel enables frequency reuse [2].

However, these interesting properties come not only with the advantage. In this frequency band, the wave is highly attenuated so that the front-end devices of the receiver-end have to be very sensitive, otherwise the radio wave will be effectively undetected. This situation thus limits the communication distance. To tackle it, increasing antenna gain is proposed allowing more margin in the link budget. Some approaches to increase the antenna gain at 60 GHz have been reported. In [3], [4], though high gain performance can be achieved, the relative large dimension and increasing complexity of the complete antenna system may limit its use, e.g. due to manufacturability and repeatability issues. This inherent limitation further prevents the feasibility of the antenna to add more features. For example to promote spectral efficiency, duplex communication by exploiting dual circular polarization is often used.

In this work, a 60-GHz dielectric rod antenna with an optimized dielectric shape to obtain the high realized gain and dual circular polarization is proposed. The antenna is not prone to rotation around its axis while facilitating the spectral efficiency. The measured gain and axial ratio bandwidth of this simpler antenna structure are higher than what is reported in [5]. This low-sidelobe rod antenna is suitable for short-range point-to-point wireless communication and automotive radar applications [6].

II. Design methodology

A. Dielectric rod antenna

The detailed dimensions of the rod are depicted in Figure 1. The rod will be fed by a patch antenna. The tapered section is to reduce the Side Lobe Level (SLL), and the uniform section is to produce maximum gain. The maximum end-fire radiation is obtained by adjusting the length of those sections. The diameter of the rod supports an HE_{11} hybrid mode if it meets the following relationship

$$D_\lambda \cong \frac{3}{\varepsilon_r^{3/2}\sqrt{1+2L_\lambda}} + 0.2, \tag{1}$$

where D_λ and L_λ are the diameter and total length of the rod in terms of free-space wavelength.

For even larger gain, smaller 3dB beamwidth and lower SLL, the cylindrical part of the dielectric can be lengthened as shown in the design template presented in [6]. To feed the antenna, low-cost 60-GHz RPC-1.85 connectors are utilized.

TPX or polymethylpentene is the material for the dielectric rod. Its relative permittivity ϵ_r and loss tangent tanδ are 2.13 and $4.8 * 10^{-4}$, respectively. The diameter of the rod base is made large to have sufficient surface area for strong adhesion. Note that the thickness of this rod base should not be larger than 0.16λ. Otherwise, though the impact is not dramatic, the realized gain will deteriorate.

B. Quadrature hybrid coupler

In Figure 2, the coupler excites the patch antenna via electromagnetic coupling to the upper layer. When port 1 is excited, the coupler acts as a 3dB power divider with a phase difference of 90°. This phase difference causes the patch to radiate circular polarization. The characteristic impedance of the through and coupling lines is $50/\sqrt{2}$ and 50Ω, respectively. The length of those lines is λ_g/4. The two arms should be electrically far from the edge of the patch to maintain the

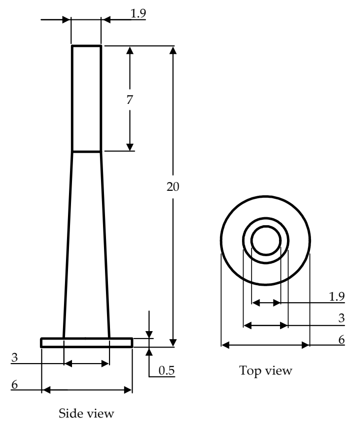

Figure 1. Dimensions of the dielectric rod. All the dimensions are in millimeter.

polarization purity of the patch radiator. The square patch antenna is used to ensure identical performances for both resulting polarization senses.

Flexible Liquid Crystal Polymer (LCP) laminate is used here and has $\epsilon_r = 3.16$ and $\tan\delta = 0.002$. The dielectric constants of the coverlay and adhesive materials used in the laminate are not available at 60 GHz. Nonetheless, it is known from the PCB manufacturer that their effective dielectric constant is approximately 3.

The 0°-plane and 90°-plane that will be used in this paper for the far-field radiation pattern are also given in Figure 2.

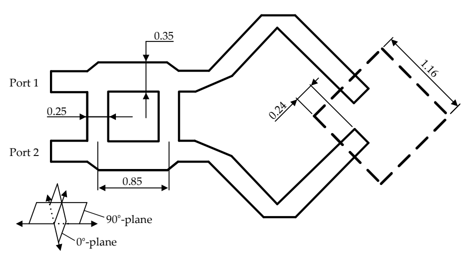

Figure 2. Dimensions of the quadrature hybrid coupler and patch antenna. All the dimensions are in millimeter.

III. Simulation and Measurement

The design and simulation are done using a full-wave EM simulator, namely CST Microwave Studio and Design Studio. The time-domain solver is employed to analyze the antenna structure.

A. Scattering parameters

The return loss of port 1 represents the reduction of signal power of the reflected wave at the antenna port in comparison with the incident wave. That reduction is attributed to the incident wave power that is radiated, partly dissipated and/or transmitted to port 2. From the S_{11} curve in Figure 3, it can be seen that the (-10dB) impedance bandwidth of the antenna system is quite broad and spans from 53 GHz up to beyond 67 GHz. On the contrary, the (-20dB) port-to-port isolation bandwidth (S_{21}) is relatively narrow, which is around 1.1 GHz.

The scattering parameters are thus interchanged as illustrated in Figure 4 and are attributed to the existence of the coupler. Due to the mismatch at the input of the antenna, the waves are reflected back at both arms. Knowing that the waves in each arm have 90° phase difference, the reflected waves that are going to the other port are constructively added whereas the other waves that are going to the exciting port are destructively added. On that account, for a proper hybrid coupler design, S_{21} herein is associated with the resonance of the antenna whereas S_{11} is basically the mutual coupling of the two arms. Likewise, the coupled waves at both arms are transmitted back to the exciting port, due to the same reason. The relatively narrow (-20dB) isolation bandwidth can thus be improved by incorporating a wideband antenna with a wideband coupler.

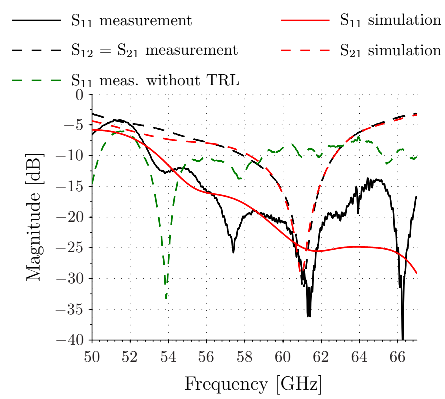

Figure 3. Scattering parameters of the antenna system.

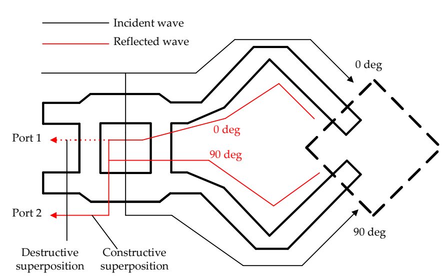

Figure 4. Illustration of the essential paths with their relative phases that cause the interchanged scattering parameters (with the assumption that the system is more antenna-limited than coupler-limited).

The antenna resonance occurs approximately at 61 GHz, and the antenna's (-20dB) isolation bandwidth is 1.1 GHz. The measurement results are in a good agreement with the simulation results. Moreover, the Thru-Reflect-Line (TRL) calibration has been performed. For that purpose, it is necessary that the 60-GHz RPC connectors with uniform impedance profiles are used. This was checked using Time Domain Reflectometry (TDR) measurement technique. With the TRL calibration, the influences of microvia, RPC connector and transmission line are de-embedded. From a simple calculation, the amount of loss of approximately 2.9 dB can be removed from the measurement.

In Figure 5, it is shown that different materials on top of the patch antenna can have a predominant effect in shifting the resonance frequency. Despite its thin dimension, the double tape

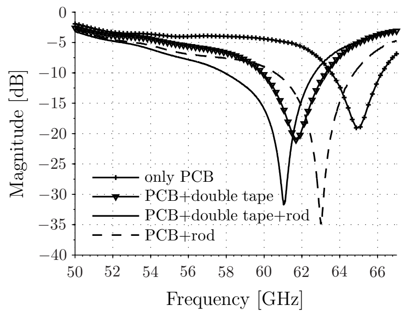

Figure 5. Measured S_{21} for step-wise integration of the patch antenna and dielectric rod.

or any kind of adhesive material, which material properties are often unavailable, may cause 2-3 GHz shift depending on its ϵ_r.

B. Radiation pattern analysis

The antenna system is designed to have circular polarization. To measure its radiation pattern, there are four methods to measure the *AR*, namely the rotating-source method, the polarization-pattern method, the phase-amplitude method and the multiple-amplitude-component method [7]. The first method is currently not available to be performed autonomously in our 60-GHz anechoic chamber. The next two methods require very accurate phase measurement, especially at 60 GHz. The last method is used here as also suggested in [8]. The measurement can be performed by rotating the linearly polarized horn antenna at 0°, 45°, 90° and -45° positions. At least three positions are already sufficient to be able to compute the polarization ellipse.

The ellipse equation eliminating the unknown semi-major and -minor axes, i.e. *a* and *b,* respectively, in polar coordinates is

$$Ae^4 - 4(A+1)e^2 + 4(A+1) = 0, \tag{2}$$

where

$$A = \frac{G_\theta^2 + G_\varphi^2 + 4\left(\frac{G_\theta G_\varphi}{G_{45}}\right)^2 - 2G_\theta G_\varphi - 4\frac{G_\theta G_\varphi^2}{G_{45}} - 4\frac{G_\theta^2 G_\varphi}{G_{45}}}{\left(G_\theta + G_\varphi\right)^2},$$

e is the eccentricity and $G_{\theta,\phi,45}$ is the antenna gain for 0°, 90°, 45° positions, respectively. Note that the gain value is not complex. The *AR* and the realized co- and cross-polarized gain of the antenna can be obtained through:

$$AR = \frac{a}{b},\ a = \frac{b}{\sqrt{1-e^2}},. \tag{3}$$

$$\begin{aligned} \max(G_{RHCP,LHCP}) &= \tfrac{G_{tot}}{2}\tfrac{(AR+1)^2}{(AR^2+1)}, \\ \min(G_{RHCP,LHCP}) &= \tfrac{G_{tot}}{2}\tfrac{(AR-1)^2}{(AR^2+1)}. \end{aligned} \tag{4}$$

The total realized gain G_{tot} is the sum of the two orthogonal components, e.g. G_θ and G_ϕ.

After the *AR* is obtained using equation (3), the realized gain of the circularly polarized antenna can be calculated by means of equation (4). The polarization mismatch is thus taken into account. The polarization sense can be observed by evaluating the field in either RHCP or LHCP wave component:

$$\begin{aligned} E_{RHCP} &= \tfrac{1}{\sqrt{2}}\left(E_\theta + jE_\phi\right) \\ E_{LHCP} &= \tfrac{1}{\sqrt{2}}\left(E_\theta - jE_\phi\right) \end{aligned}. \tag{5}$$

E_θ and E_ϕ are the fields from any two orthogonal cuts, e.g. E_0 and E_{90}, respectively. Note that the fields are complex. By looking which absolute field is largest for $\theta = 0$, the polarization sense can be determined.

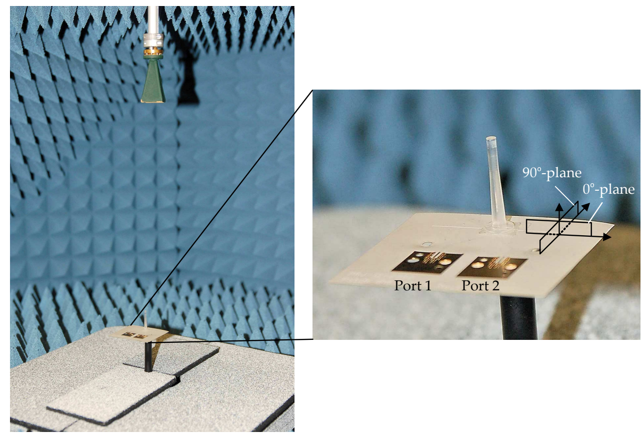

(a) (b)

Figure 6. (a) The 60-GHz anechoic chamber and (b) the dielectric rod antenna.

In Figure 6, the measurement facility and manufactured dielectric rod antenna are depicted. It can be seen at the top that the linearly polarized horn antenna is used for the measurement of the radiation pattern and at the bottom the manufactured dielectric rod antenna is positioned. The footprints for attaching two RPC connectors are shown in Figure 6(b).

From Figure 7, it is clear that the shapes of the measured co-polar pattern and *AR* pattern agree with the simulated ones. Also the measured antenna gain is as simulated with achieved 14.6dBi gain for $\theta = 0$, but the measured *AR* is slightly better than the simulated one.

From the measurement, E_{LHCP} has a lower value than E_{RHCP}, especially in the direction of the main lobe. Hence, the antenna radiation has right-hand circular polarization as predicted from the simulation.

The measurement results in the 90°-plane are also in good agreement with the simulation results (see in Figure 8). From the observation for $\theta < 0°$, the waves are influenced by the RPC connectors and termination load (obstacles) which slightly shift the lobe's maxima and minima. For $\theta > 0°$, the smaller as predicted *AR* is partly responsible for these higher side lobes.

In Figure 9, the (-20dB) isolation bandwidth is illustrated. Hence, the useful antenna performance is measured for the bandwidth of 1.1 GHz.

In Figure 10, the performance of the dielectric rod antenna is summarized for both 0°-plane and 90°-plane. It can be observed that the obtained gain is around 15 dBi. The *AR* in the frequency band of interest is below 0.5 dB. Although it is not mentioned here for brevity, the 3dB *AR* bandwidth

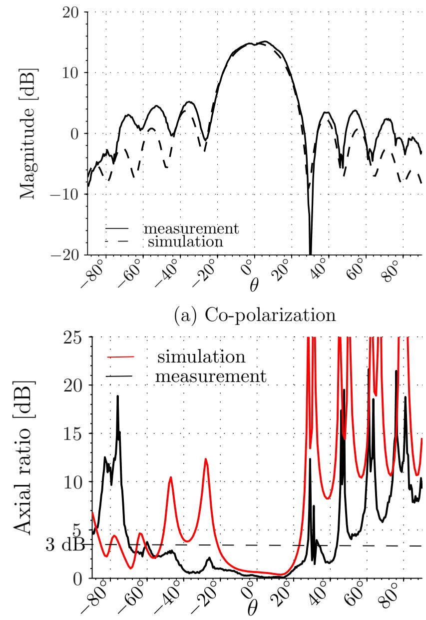

(a) Co-polarization

(b) Axial ratio AR

Figure 7. Radiation patterns in the 0°-plane at 61 GHz for (a) Co-polarization pattern (with achieved 14.6dBi gain) and (b) axial ratios in the 0°-plane

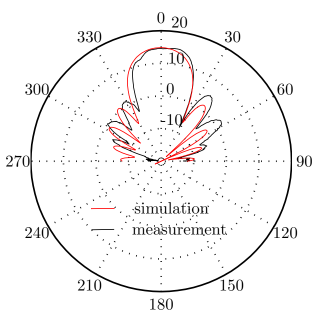

Figure 8. RHCP radiation patterns in the 90°-plane at 61 GHz.

covers the whole 60-GHz ISM band. This is mainly due to the use of the quadrature hybrid coupler. The 3dB beamwidth for both principle planes is similar over the frequency band, showing the symmetry property of the rod's radiation pattern. The sidelobe level is measured to be around -9.5 dB.

IV. Conclusion

The dielectric rod antenna with dual circular polarization has been designed, manufactured and measured. The resonance peak occurs around 61 GHz, and a 15dBi circularly-polarized antenna gain is realized. The measured radiation pattern has right-hand circular polarization. The port-to-port (-20dB) isolation bandwidth is 1.1 GHz. This high port-to-port isolation of the antenna enables duplex communication with reduced complexity of the RF front-end devices, e.g. it avoids the use of a duplex filter or a switch. Further, the antenna structure is easy and low cost to manufacture and can support the short-range point-to point-communication and automotive applications.

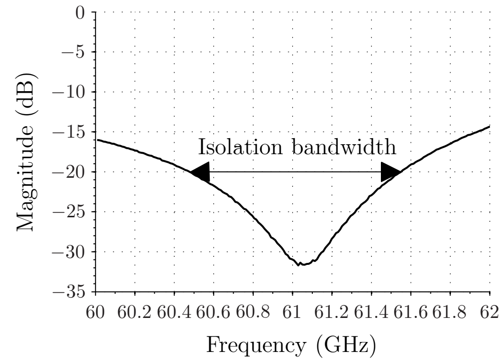

Figure 9. Definition of (-20dB) isolation bandwidth from S_{21} measurement. Note that -20dB isolation means -20dB coupled to port 2.

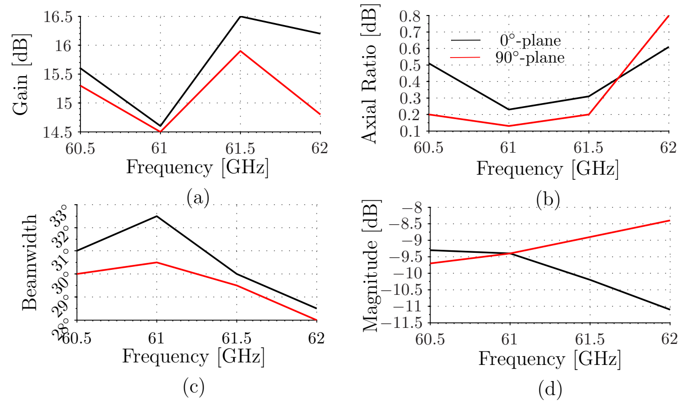

Figure 10. Measured antenna performance over the frequency band of interest (i.e. (-20dB) isolation bandwidth from 60.45 - 61.55 GHz). (a) Co-polarization gain, (b) Axial ratio, (c) 3dB beamwidth, and (d) SLL.

Acknowledgement

The authors would like to thank A.C.F. Reniers for the valuable support in the measurement.

References

[1] S. Cherry, "Edholm's law of bandwidth," *IEEE Spectrum*, vol. 41, no. 7, pp. 58 – 60, July 2004.

[2] P. Smulders, "Exploiting the 60 GHz band for local wireless multimedia access: Prospects and future directions," *IEEE Communications Magazine*, vol. 40, no. 1, pp. 140 –147, Jan. 2002.

[3] M. Al Henawy and M. Schneider, "Planar antenna arrays at 60 GHz realized on a new thermoplastic polymer substrate," in *2010 Proceedings of the Fourth European Conference on Antennas and Propagation (EuCAP)*, April 2010, pp. 1 –5.

[4] N. Caillet, C. Person, C. Quendo, J. Favennec, S. Pinel, E. Rius, and J. Laskar, "High gain conical horn antenna integrated to a planar substrate for 60 GHz WPAN applications," in *2010 Proceedings of the Fourth European Conference on Antennas and Propagation (EuCAP)*, April 2010, pp. 1 –5.

[5] K.-C. Huang and Z. Wang, "V-band patch-fed rod antennas for high data-rate wireless communications," *IEEE Transactions on Antennas and Propagation*, vol. 54, no. 1, pp. 297 – 300, Jan. 2006.

[6] M. Rousstia, *Switched-beam antenna array design for millimeter-wave applications*. PDEng Report, SAI-ICT, Eindhoven University of Technology, 2011.

[7] *IEEE Standard Test Procedures for Antennas*, ANSI/IEEE Std 149-1979 Std., 1979.

[8] D. Titz, F. Ferrero, and C. Luxey, "Development of a millimeter-wave measurement setup and dedicated techniques to characterize the matching and radiation performance of probe-fed antennas [measurements corner]," *IEEE Antennas and Propagation Magazine*, vol. 54, no. 4, pp. 188 –203, Aug. 2012.